International Journal of Control, Automation and Systems 16(4) (2018) 1814-1823
http://dx.doi.org/10.1007/s12555-017-0509-0
ISSN:1598-6446 eISSN:2005-4092
http://www.springer.com/12555

Finite-time Controller Design for Four-wheel-steering of Electric Vehicle Driven by Four In-wheel Motors

Qinghua Meng*, Zong-Yao Sun, and Yushan Li

Abstract: A smooth control method may do not obtain a desired convergence. On the other hand, a no-continuous method may cause a close-loop system to chatter. In order to avoid the aforementioned disadvantages, a non-smooth finite-time control method is proposed and applied on an active four-wheel-steering electric vehicle driven by four in-wheel motors to improve the safety and manoeuvrability in this paper. Based on an ideal electric vehicle steering tracking model, a non-smooth finite-time convergence controller is constructed for controlling the four wheels' steering angles of an electric vehicle. The front wheel cornering stiffness, rear wheel cornering stiffness and external disturbance of a practical car are regarded as bounded uncertain parameters according to practical conditions. An A-class car model in the Carsim software is utilized to simulate the designed controller. The simulation results show that the controller based on finite-time convergence can track the ideal vehicle steering model better to obtain zero sideslip angle and expected yaw rate even when there exist perturbation of cornering stiffness and disturbance of lateral wind. It means the control system of the electric vehicle is robust with uncertainty. The simulation results also show that the non-smooth finite-time control method is better than the slide mode control method for the active four-wheel-steering system of the electric vehicle.

Keywords: Electric vehicle, finite-time convergence, four-wheel-steering, stability control.

1. INTRODUCTION

The four-wheel-steering system is employed by some cars to improve steering response, and increase vehicle maneuvering stability under high speed, or decrease turning radius under low speed. In an active four-wheel steering system, all four wheels turn at the same time when a car steers. The four-wheel-steering (4WS) is a core control technology for the active vehicle chassis which is becoming more and more interesting for improving safety and manoeuvrability of a car. With the development of the EV driven by four in-wheel motors, the four-wheel-steering technology is improved correspondingly. The active four-wheel-steering system can control the yaw and lateral motion by the front wheels and rear wheels to reduce the steering force delay, and control the motion trajectory and attitude independently for lateral stability when an EV turns [1–4]. The smooth control method has been used for four-wheel-steering widely, but it's convergence performance is not perfect, and it is not a time optimal control method [5–10]. The variable structure control theory is applied for the vehicle by more and more researchers [11, 12]. The slide mode variable structure control has fast convergence and anti-disturbance performance, but it is asymptotically stable and uncontinuous, which may lead to chattering in a closed-loop system [13–17]. Now, the adding power integer, finite-time convergence and high order slide mode control are introduced into the slide mode control method, which differ from the classic slide mode control [18–21]. In fact, the finite-time convergence method is a kind of feedback control method which is between the smooth method and uncontinuous feedback method, and the controller based on the finite-time convergence method can track target within finite time with strong robustness and without chattering [22–28]. By the way, some fuzzy-model-based approximation methods have been proposed to characterize the nonlinear model to deal with parameter uncertainties [29–32].

In order to solve the aforementioned problems, an uncertain four-wheel-steering model is proposed in this paper which considers the bounded uncertain front wheel

Manuscript received August 25, 2017; revised November 26, 2017; accepted December 14, 2017. Recommended by Associate Editor Sing Kiong Nguang under the direction of Editor Hamid Reza Karimi. This research were supported by Zhejiang Provincial Natural Science Foundation of China under Grant No. LY16E050003, National Natural Science Foundation of China under Grant 61773237, and China Postdoctoral Science Foundation Funded Project under grant 2017M610414.

Qinghua Meng is with the School of Mechanical Engineering, Hangzhou Dianzi University, Hangzhou 310018, China (e-mail: mengqinghua@hdu.edu.cn). Zong-Yao Sun is with the Institute of Automation, Qufu Normal University, Qufu 273165, China (e-mail: sunzongyao@sohu.com). Yushan Li is with the College of Transportation, Shandong University of Science and Technology, Qingdao 266590, China (e-mail: skd_lys@163.com).
* Corresponding author.

cornering stiffness, rear wheel cornering stiffness and external disturbances. And an ideal tracking model is established also for constructing a non-smooth finite-time convergence controller to track the desired sideslip angle and yaw rate. Then a vehicle controller, based on the vehicle ideal tracking model and uncertain four-wheel -steering model, is designed to track the desired values using the non-smooth finite-time convergence method. Finally, the controller is simulated by the Matlab and Carsim software to verify the controller's efficiency.

Compared with the prior studies, innovations of this paper lie in the following aspects.

1) The 4WS model includes bounded uncertain front wheel cornering stiffness, rear wheel cornering stiffness and external disturbances.
2) An error tracking model of the 4WS is constructed for active 4WS stability controlling.
3) A non-smooth finite-time controller for the uncertain 4WS of an EV driven by four in-wheel motors is proposed.

2. THE STEERING DYNAMIC MODEL OF AN EV

2.1. The four-wheel-steering dynamic model

In this paper, we will establish a linear 2 Degree of Freedom (2DOF) 4WS model which includes the sideslip angle, yaw rate, front wheel angle and rear wheel angle. Some assumptions are proposed before the model is established.

Assumption 1: the influence of the steering system is ignored, and the front wheel angle is the system input.

Assumption 2: the pitch motion and roll motion are ignored, and the EV is assumpted to just move along longitudinal direction. Then the EV just has 2DOF which are lateral motion and yaw motion. Forces analysis of the 4WS model based on the aforementioned assumptions is shown in Fig. 1.

The kinematic model based on the aforementioned assumptions is shown in Fig. 2.

According to Figs. 1 and 2, the mathematical model of the 4WS is

$$\begin{aligned}
&m\frac{v^2}{\rho}\sin\beta - m\dot{v}\cos\beta + F_{xr}\cos\delta_r + F_{yr}\sin\delta_r - F_{wx} \\
&\quad + F_{xf}\cos\delta_f - F_{yf}\sin\delta_f = 0, \\
&m\frac{v^2}{\rho}\cos\beta - m\dot{v}\sin\beta + F_{xr}\sin\delta_r - F_{yr}\cos\delta_r - F_{wy} \\
&\quad - F_{xf}\sin(\delta_f) - F_{yf}\cos(\delta_f) = 0, \\
&I_z\dot{\dot{\varphi}} - (F_{yf}\cos\delta_f + F_{xf}\sin\delta_f)a + (F_{yr}\cos\delta_r \\
&\quad - F_{xr}\sin\delta_r)b - F_{wy}l_w = 0,
\end{aligned} \tag{1}$$

where m is the mass of the car, v is the longitudinal velocity of centroid, ρ is the turning radius, β is the sideslip angle, γ is the yaw rate, δ_f and δ_r are the front wheel angle and rear wheel angle respectively, F_{xf} is the front wheel longitudinal force, F_{xr} is the rear wheel longitudinal force, F_{yf} is the front wheel lateral force, F_{yr} is the rear wheel lateral force, F_{wx} is the lateral wind longitudinal force, F_{wy} is the lateral wind lateral force, I_z is the rotary inertia around Z axis, a and b are the distances from centroid to the front axle and rear axle respectively, l_w is the distance from the vehicle centroid to the lateral wind force centre.

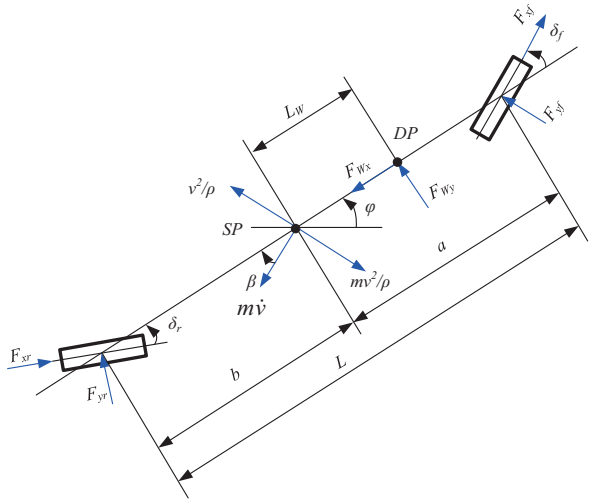

Fig. 1. The forces analysis of the 4WS model of an EV driven by four in-wheel motors.

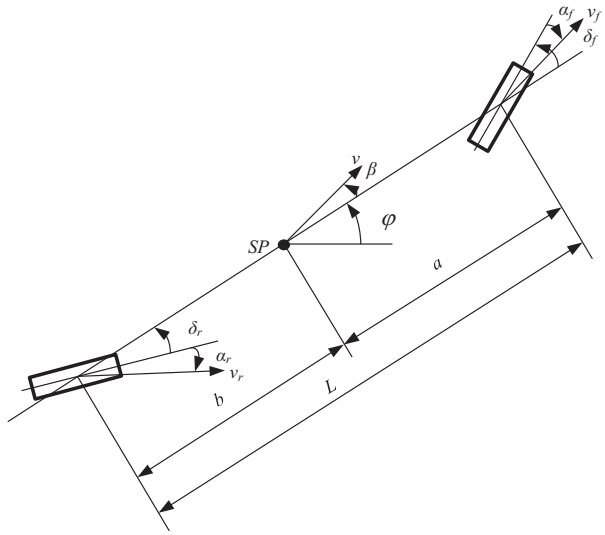

Fig. 2. The 4WS dynamic model of an EV driven by four in-wheel motors.

Considering the yaw rate along the vehicle longitudial axle, there exist

$$\begin{aligned}
v_f\sin(\delta_f - \alpha_f) &= a\dot{\varphi} + v\sin\beta, \\
v_r\sin(\delta_r + \alpha_r) &= b\dot{\varphi} - v\sin\beta,
\end{aligned} \tag{2}$$

where v_f and v_r are the velocities of the front wheel and rear wheel respectively, α_f and α_r are front tire sideslip angle and rear tire sideslip angle respectively, φ is the yaw angle.

Assumping $v = v_f = v_r$, we obtain the following equation from (2),

$$\begin{aligned}\tan(\delta_f - \alpha_f) &= \frac{a\dot{\varphi} + v\sin\beta}{v\cos\beta},\\ \tan(\delta_r + \alpha_r) &= \frac{b\dot{\varphi} - v\sin\beta}{v\cos\beta}.\end{aligned} \tag{3}$$

When the angles are small, there exist

$$\begin{aligned}\alpha_f &= -\beta + \delta_f - a\frac{\dot{\varphi}}{v},\\ \alpha_r &= -\beta - \delta_r + b\frac{\dot{\varphi}}{v}.\end{aligned} \tag{4}$$

We select the linearized functions for tire forces and sideslip angles which are

$$\begin{aligned}F_{yf} &= 2k_1\alpha_f,\\ F_{yr} &= 2k_2\alpha_r,\end{aligned} \tag{5}$$

where k_1 and k_2 are the front tire cornering stiffness and rear tire cornering stiffness respectively.

Substituting (4) and (5) into (1), one obtains

$$\begin{aligned}mv\dot{} &= F_{xf} + F_{xr} - F_{Wx},\\ mv(\dot{\beta} + \dot{\varphi}) + m\dot{v}\beta &= 2k_1(-\beta + \delta_f - a\frac{\dot{\varphi}}{v})\\ &\quad + 2k_2(\beta - \delta_r - b\frac{\dot{\varphi}}{v}) + F_w,\\ I_z\ddot{\varphi} &= 2k_1a(-\beta + \delta_f - a\frac{\dot{\varphi}}{v})\\ &\quad - 2k_2b(-\beta - \delta_r + b\frac{\dot{\varphi}}{v}) - F_wl_w.\end{aligned} \tag{6}$$

When $\dot{v} = 0$, and define $\gamma = \dot{\varphi}$, Equ.(6) is rewritten as

$$\begin{aligned}\dot{\beta} &= -\frac{2(k_1+k_2)}{mv}\beta - (\frac{2(ak_1 - bk_2)}{mv^2} + 1)\gamma\\ &\quad + \frac{2k_1}{mv}\delta_f - \frac{2k_2}{mv}\delta_r + \frac{F_w}{mv},\\ \dot{\gamma} &= -\frac{2(ak_1 - bk_2)}{I_z}\beta - \frac{2(a^2k_1 + b^2k_2)}{v}\gamma\\ &\quad + \frac{2ak_1}{I_z}\delta_f + \frac{2bk_2}{I_z}\delta_r + \frac{F_wl_w}{I_z},\end{aligned} \tag{7}$$

where F_w is the external disturbance force.

Then we can obtain the state space equations of system (7)

$$\begin{cases}\dot{X} = AX + BU + GD,\\ Y = CX,\end{cases} \tag{8}$$

where

$$A = \begin{bmatrix} -2\frac{k_1+k_2}{mv} & -2\frac{ak_1-bk_2}{mv^2} - 1\\ -2\frac{ak_1-bk_2}{I_z} & -2\frac{a^2k_1+b^2k_2}{v}\end{bmatrix},\ C = \begin{bmatrix}1 & 0\\ 0 & 1\end{bmatrix},$$
$$B = \begin{bmatrix} 2\frac{k_1}{mv} & -2\frac{k_2}{mv}\delta_r\\ 2\frac{ak_1}{I_z} & 2\frac{bk_2}{I_z}\end{bmatrix}, G = \begin{bmatrix}\frac{1}{mv}\\ -\frac{l_w}{I_z}\end{bmatrix},$$
$$X = \begin{bmatrix}\beta\\ \gamma\end{bmatrix}, U = \begin{bmatrix}\delta_f\\ \delta_r\end{bmatrix}, D = F_w.$$

2.2. The uncertain 4WS model of an EV

When an EV runs, the tire cornering stiffness is variable but bounded under different conditions . Then k_1 and k_2 are defined as the nominal values of the front wheel cornering stiffness and rear wheel cornering stiffness, and Δk_1 and Δk_2 are perturbations respectively. The state space equations of system (7) is

$$\dot{X} = (A_0 + \Delta A)X + (B_0 + \Delta B)U + GD, \tag{9}$$

where

$$A_0 = \begin{bmatrix} -2\frac{k_{01}+k_{02}}{mv} & -2\frac{ak_{01}-bk_{02}}{mv^2} - 1\\ -2\frac{ak_{01}-bk_{02}}{I_z} & -2\frac{a^2k_{01}+b^2k_{02}}{v}\end{bmatrix},$$
$$B_0 = \begin{bmatrix} 2\frac{k_{01}}{mv} & -2\frac{k_{02}}{mv}\\ l_fC_{f0}h_0 & h_0\end{bmatrix},$$
$$\Delta A = \begin{bmatrix} -2\frac{\Delta k_1+\Delta k_2}{mv} & -2\frac{a\Delta k_1-b\Delta k_2}{mv^2}\\ -2\frac{a\Delta k_1-b\Delta k_2}{I_z} & -2\frac{a^2\Delta k_1+b^2\Delta k_2}{v}\end{bmatrix},$$
$$\Delta B = \begin{bmatrix} 2\frac{\Delta k_1}{mv} & -2\frac{\Delta k_2}{mv^2}\\ 2\frac{a\Delta k_1}{I_z} & 2\frac{b\Delta k_2}{I_z}\end{bmatrix},$$
$$X = \begin{bmatrix}\beta\\ \gamma\end{bmatrix}, U = \begin{bmatrix}\delta_f\\ \delta_r\end{bmatrix}, G = \begin{bmatrix}\frac{1}{mv}\\ -\frac{l_w}{I_z}\end{bmatrix},$$
$$D = F_w.$$

2.3. The ideal tracking 4WS model of an EV

An ideal 4WS tracking model should keep the steering sensitivity of an EV as same as a traditional car, and make the sideslip angle tend to zero after adding a rear wheel angle. Then the ideal tracking model can be constructed as

$$\dot{X}_d = A_dX_d + B_dU_d, \tag{10}$$

where

$$X_d = \begin{bmatrix}\beta_d\\ \gamma_d\end{bmatrix},\ A_d = \begin{bmatrix}0 & 0\\ 0 & -1/\tau_{rd}\end{bmatrix},$$
$$B_d = \begin{bmatrix}0\\ \kappa_{rd}/\tau_{rd}\end{bmatrix},\ U_d = u_f^*.$$

In (10), X_d is the state vector of the ideal model, U_d is the input, β_d and γ_d are the ideal sideslip angle and yaw rate respectively, k_{rd} is the yaw rate steady gain of the FWS, τ_{rd} is a time constant of one-order inertia.

3. DESIGN OF THE NON-SMOOTH FINITE-TIME CONVERGENCE CONTROLLER

3.1. The matching condition

Define

$$M_1 = \begin{bmatrix} -\lambda_f & -\frac{a}{v}\lambda_f \\ \lambda_r & -\frac{b}{v}\lambda_r \end{bmatrix}, M_2 = \begin{bmatrix} \lambda_f & 0 \\ 0 & \lambda_r \end{bmatrix}, \quad (11)$$

$$M_3 = \begin{bmatrix} \eta_f \\ \eta_r \end{bmatrix},$$

where

$$\begin{cases} \lambda_f = \Delta k_1/k_{10} \\ \lambda_f = \Delta k_2/k_{20}, \end{cases} \quad \begin{cases} \eta_f = (b-l_w)/(k_{10}L) \\ \eta_r = (a+l_w)/(k_{20}L). \end{cases}$$

Then

$$\Delta A = B_0 M_1, \Delta B = B_0 M_2, G = B_0 M_3. \quad (12)$$

Equation (12) means that the 4WS model meets the matching condition. We define $f(x,t)$ to be uncertainty, then

$$\begin{aligned} f(x,t) &= \Delta AX + \Delta BU + GD \\ &= B_0(M_1X + M_2U + M_3D) = B_0 d(x,t), \end{aligned} \quad (13)$$

where

$$d(x,t) = \begin{bmatrix} d_1(x,t) \\ d_2(x,t) \end{bmatrix} = M_1X + M_2U + M_3D\,.$$

Then, (8) is rewritten as

$$\dot{X} = A_0X + B_0\left[U + d(x,t)\right]. \quad (14)$$

There exist parameter perturbation and external disturbances in practice. A suitable control method can eliminate the influence of the uncertainty according to the matching condition. The finite-time convergence control method, being the non-smooth control theory, can converge the tracking error of the system to zero and do not generate chattering to damage the actuators. And the method is strongly robust which make the system response to be not sensitive for uncertainty. Therefore, we apply this method into the 4WS control system, and design the 4WS control system, as shown in Fig. 3. The tracking error e is

$$e = X_d - X = \begin{bmatrix} \beta_d - \beta & \gamma_d - \gamma \end{bmatrix}^T. \quad (15)$$

Then

$$\dot{e} = A_d e + (A_d - A_0)X + B_d U_d - B_0\left[U + d(x,t)\right]. \quad (16)$$

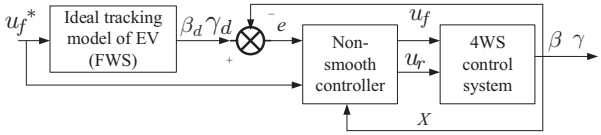

Fig. 3. The diagram of the non-smooth 4WS control system.

3.2. Design of the non-smooth finite-time convergence controller

There always exist disturbances in the practical 4WS system. The slide mode control method can ensure vectors to reach a sliding surface within finite time. But the target tracking error can not reach zero. A finite-time controller can stabilize the target tracking error within a small interval and to reach zero. The finite-time stabilization is defined as

$$\dot{x} = f(x),\ \ x \in U \subseteq R^n,\ \ f(0) = 0, \quad (17)$$

where $f : U \to R^n$ is a continuous function for x in the open domain U, and the origin is included in the U. $x = 0$ is finite-time stable if and only if the system is strong stability and finite-time convergence. Finite-time convergence means that there is a continuous function $T(x), U_0\backslash 0 \in (0,+\infty), \forall x_0 \in U_0 \subset R^n$, which can keep $x(t,x_0)$ meet $x(t,x_0) \in U_0\backslash 0$ and $\lim_{t\in T(x_0)} x(t,x_0) = 0$ when $t \in [0, T(x_0))$, and $x(t,x_0) = 0$ when $t > T(x_0)$. The system is globally finite-time stable if $U = U_0 = R^n$.

According to the 4WS model, the finite-time convergence controller is designed as

$$\begin{aligned} U =& B_0^{-1}A_d e\varepsilon \mathrm{sgn}(e)|e|^\alpha \\ &+ B_0^{-1}(A_d - A_0)X + B_d U_d \varepsilon \mathrm{sgn}(e)|e|^\alpha \\ =& U_{eq} + U_{sw}, \end{aligned} \quad (18)$$

where $\varepsilon \mathrm{sgn}(e)|e|^\alpha = [\varepsilon_1 \mathrm{sgn}(e_1)|e_1|^{\alpha_1} \quad \varepsilon_2 \mathrm{sgn}(e_2)|e_2|^{\alpha_2}]^T$, $\varepsilon_1 > 0, \varepsilon_2 > 0, 0 < \alpha_1 < 1, 0 < \alpha_2 < 1$.

The designed controller is constructed by two parts. One is the linear continuous feedback equivalent control part U_{eq}, and the other is non-smooth nonlinear feedback switch control part U_{sw} which is used to deal with the uncertainties of the system.

3.3. Analysis of anti-disturbance

Substituting (18) into (16), one obtains the tracking error function

$$\dot{e} = -\varepsilon \mathrm{sgn}(e)|e|^\alpha + B_0 d(x,t), \quad (19)$$

where $e = [e_1 \quad e_2]^T$, e_1 is the sideslip angle tracking error, e_2 is the yaw rate tracking error.

Define

$$B_0 = \begin{bmatrix} b_{11} & b_{12} \\ b_{21} & b_{22} \end{bmatrix}, \quad (20)$$

then

$$\begin{aligned} \dot{e_1} &= -\varepsilon_1 \mathrm{sgn}(e_1)|e_1|_1^{\alpha} + b_{11}d_1(x,t) + b_{12}d_2(x,t), \\ \dot{e_2} &= -\varepsilon_2 \mathrm{sgn}(e_2)|e_2|_2^{\alpha} + b_{21}d_1(x,t) + b_{22}d_2(x,t). \end{aligned} \tag{21}$$

For convenience, we define

$$\begin{aligned} \acute{d_1}(x,t) &= b_{11}d_1(x,t) + b_{12}d_2(x,t), \\ \acute{d_2}(x,t) &= b_{21}d_1(x,t) + b_{22}d_2(x,t). \end{aligned} \tag{22}$$

According to Equ.(13) and Equ.(11), in a practical EV, there exists

$$\begin{aligned} d_1(x,t) &= -\lambda_f\beta - \frac{a}{v}\lambda_f\gamma + \lambda_f u_f + \eta_f F_W \\ &\le |\bar{\lambda_f}||\bar{\beta}| - \frac{a}{\underline{v}}|\bar{\lambda_f}||\bar{\gamma}| + \eta\bar{u_f}| = l_1, \end{aligned} \tag{23}$$

where $|\bar{\lambda}_f|$, $|\bar{\beta}|$, $|\bar{\gamma}|$ and $\bar{u_f}$ are the upper limit absolute values of λ_f, β, γ and u_f respectively. $\underline{v}$ is the lower limit value of v. In the same way, $d_2(x,t) \le l_2$. Therefore, the disturbances are bounded, that is to say

$$|d_1(x,t)| \le l_1, \;\; |d_2(x,t)| \le l_2; \;\; \forall t \ge 0, \tag{24}$$

where $l_1 > 0$, $l_2 > 0$.

Then

$$\begin{aligned} |b_{11}d_1(x,t) + b_{12}d_2(x,t)| \le & |b_{11}||d_1(x,t)| \\ & + |b_{12}||d_2(x,t)| \\ \le & |b_{11}|l_1 + |b_{12}|l_2 \\ = & \acute{l_1}, \\ |b_{21}d_1(x,t) + b_{22}d_2(x,t)| \le & |b_{21}||d_1(x,t)| \\ & + |b_{22}||d_2(x,t)| \\ \le & |b_{21}|l_1 + |b_{22}|l_2 \\ = & \acute{l_2}. \end{aligned} \tag{25}$$

Therefore, $\acute{d_1}(x,t)$ and $\acute{d_2}(x,t)$ are bounded, that is to say

$$|\acute{d_1}(x,t)| \le \acute{l_1}, |\acute{d_2}(x,t)| \le \acute{l_2}, \forall t \ge 0, \tag{26}$$

where $\acute{l_1} > 0$ and $\acute{l_2} > 0$.

Next, we will give a theorem to describe the main result of this paper.

Theorem 1: If the external disturbances are bounded, there is a controller (18) to stabilize the sideslip angle tracking error and yaw rate tracking error within intervals Q_1 and Q_2,

$$\begin{aligned} Q_1 &= \left\{ e_1 : |e_1| \le \left((\acute{l_1} + c_1)/\varepsilon_1 \right)^{1/\alpha_1} \right\}, \\ Q_2 &= \left\{ e_2 : |e_2| \le \left((\acute{l_2} + c_2)/\varepsilon_2 \right)^{1/\alpha_2} \right\}, \end{aligned} \tag{27}$$

where $c_1 > 0$, $c_2 > 0$, $\varepsilon_1 > 0$, $\varepsilon_2 > 0$, $0 < \alpha_1 < 1$, $0 < \alpha_2 < 1$.

Proof: According to (19), there exists

$$\dot{e} = -\varepsilon \mathrm{sgn}(e)|e|^{\alpha} + B_0 d(x,t). \tag{28}$$

The Lyapunov function is constructed as

$$V(e_1) = e_1^2/2. \tag{29}$$

The derivative of (29) is

$$\begin{aligned} \dot{V}(e_1) = e_1\dot{e}_1 &\le -\varepsilon_1|e_1|^{1+\alpha_1} + \acute{l_1}|e_1| \\ &= -(\varepsilon_1|e_1|^{\alpha_1} - \acute{l_1})|e_1|. \end{aligned} \tag{30}$$

Note

$$Q_1 = \left\{ e_1 : |e_1| \le \left((\acute{l_1} + c_1)/\varepsilon_1 \right)^{1/\alpha_1} \right\}, \tag{31}$$

where $c_1 > 0$ is a constant. Then one can get

$$R - Q_1 = \left\{ e_1 : |e_1| > \left((\acute{l_1} + c_1)/\varepsilon_1 \right)^{1/\alpha_1} \right\}. \tag{32}$$

Because of (29), it is easy to verify that for $e \in R - Q_1$,

$$\frac{1}{2}e_1^2 > \frac{1}{2}\left(\frac{\acute{l_1} + c_1}{\varepsilon_1} \right)^{2/\alpha_1}. \tag{33}$$

Then we obtain

$$|e_1| > \left(\frac{\acute{l_1} + c_1}{\varepsilon_1} \right)^{1/\alpha_1}. \tag{34}$$

Combing (30) and (34), one obtains

$$\dot{V}(e_1) < -c_1 \left(\frac{\acute{l_1} + c_1}{\varepsilon_1} \right)^{1/\alpha_1} < 0. \tag{35}$$

There are two cases for the original value $e_1(0)$. The first one is that the original value is out of Q_1, i.e., $e_1(0) \in R - Q_1$. Because of (35), there exists $t_1 > 0$ leading to

$$e_1(t_1) \in \partial Q_1 = \left\{ e_1 : V(e_1) = \frac{1}{2}\left(\frac{\acute{l_1} + c_1}{\varepsilon_1} \right)^{2/\alpha_1} \right\}, \tag{36}$$

where ∂Q_1 is defined as the boundary of Q_1. The other is the original value is within Q_1, i.e., $e_1(0) \in Q_1$. If $e_1(t)$ is always within Q_1, it is not necessary to prove it's convergence. Therefore, we just discuss the case of $e_1(t)$ fleeing from Q_1. Under this case, there still exists $t_1 > 0$ to meet $e_1(t_1) \in \partial Q_1$. Next, we will prove $e_1(t) \in Q_1$ for any $t \in [t_1, +\infty)$.

Note

$$m = \inf_{e_1(t) \in \partial Q_1} V(e_1), \tag{37}$$

and

$$p = \inf_{e_1(t)\in\partial Q_1} (\varepsilon_1 |e_1|^{1+\alpha_1} - l|e_1|). \tag{38}$$

Then it is easy to obtain

$$m = \frac{1}{2}\left(\frac{\acute{l_1}+c_1}{\varepsilon_1}\right)^{2/\alpha_1}, \tag{39}$$

and

$$p = c_1\left(\frac{\acute{l_1}+c_1}{\varepsilon_1}\right)^{2/\alpha_1}, \tag{40}$$

where $p > 0$. Because $V(e_1)$ is continuous, for $e_1(t) \in \partial Q_1$, there exists

$$\dot{V}(e_1(t)) \le -p < 0. \tag{41}$$

Then we can derive that there exists $s_1 > 0$ to make $t \in [t_1, t_1 + s_1)$, and $e_1(t) \in Q_1$. Assuming that $e_1(t)$ will flee from Q_1 , which leads to existing $h_1 \in [t_1, +\infty)$ to make $e_1(h_1) \bar{\in} Q_1$. It means there is a $\delta \in (t_1, h_1)$ to make $e_1(\delta) \in \partial Q_1$. Because $\dot{V}(e_1(\delta)) \le -p < 0$, and $V(e_1)$ is continuous, there exists s_2 to make $V(e_1(t))$ being nonincreasing within $[\delta - s_2, \delta)$ that leads to an impossible result for $m = V(e_1(\delta)) < m$. Therefore, $t \in [t_1, +\infty)$ meets

$$|e_1(t)| \le \left(\frac{\acute{l_1}+c_1}{\varepsilon_1}\right)^{1/\alpha_1}. \tag{42}$$

The aforementioned information means that the sideslip angle tracking error of the uncertain 4WS model can converge in finite time. In the same way, it can be proved that the yaw rate tracking error of the uncertain 4WS model can converge in finite time also.

4. SIMULATION ANALYSIS

In this paper, an A-class car model in the Carsim software is used to simulate the controller. The vehicle parameters are listed in Table1. In this paper, the finite-time convergence controller for the 4WS system and the FWS are simulated by the double lane closed-loop test to verify the efficiency of the controller. The simulation results without external disturbance under 90 km/h are shown in Fig. 4. Fig. 4 shows that the 4WS controller can track the desired yaw rate better than two wheel steering system. The sideslip angle converges to zero under the straight running condition, and a very small fluctuation under the lane-change condition with the 4WS controller. The sideslip angle of the traditional two wheel steering system fluctuates along the line. The results show that 4WS finite-time convergence controller has better robustness for parameters perturbation, and can track the desired values to improve the lateral stability greatly.

Table 1. Vehicle parameters.

Parameters	Value
The rotary inertia I_z/kg·m^2	2031.4
The mass m/kg	1111
The length between front axle and centroid a/m	1.04
The length between rear axle and centroid b/m	1.56
The lateral stiffness of front axle k_1/N·rad^{-1}	80255
The lateral stiffness of rear axle k_2/N·rad^{-1}	57325

Then, a disturbance, 100N lateral wind force, is applied to the point being away from the the center of mass to simulate the 4WS control system. The simulation results are shown in Fig. 5. Fig. 5 shows that the 4WS controller still can track the desired line better than 2WS, and the lateral displacement bias is just 0.04m compared with the lateral displacement bias of 2WS being 0.06m. The 4WS controller can track the desired yaw rate better than 2WS with lateral wind force also. Compared with 2WS, the sideslip angle of 4WS has a very small fluctuation and tends to zero under the external lateral wind force. The results show that the 4WS system with the designed controller has stronger adaption for the external disturbance and parameters perturbation than 2WS, which improves the robustness of an EV and helps dirvers to deal with danger conditions for safety.

In this paper, the simulation results under the slide mode control method and non-smooth control method are compared, as shown in Fig. 6. From Fig. 6(a) and Fig. 6(b), we know that the non-smooth control method and slide mode control method are both have identical control results for the lateral displacement and the yaw rate. According to Fig. 6(c), it is obvious that the non-smooth control method has better control performance than the slide mode control method for the sideslip angle. From Fig. 6(d) and Fig. 6(e), we can see that the slide mode control method generates chattering. The simulation results under the non-smooth control method are better than the slide mode control for the four wheel angles.

5. CONCLUSION

In this paper, an active 4WS control model is built for an EV driven by four-wheel motors, and a finite-time convergence controller is designed based on the model. The theory analysis shows that the designed controller has good robustness against parameter perturbation and uncertainty. The simulation is carried out by Simulink and Carsim softwares to verify that the designed 4WS finite-time convergence controller can track the desired model, eliminate some uncertainties, and keep the sideslip angle being zero to improve the system robustness and driving safety. Compared with the slide mode control method, the simulation

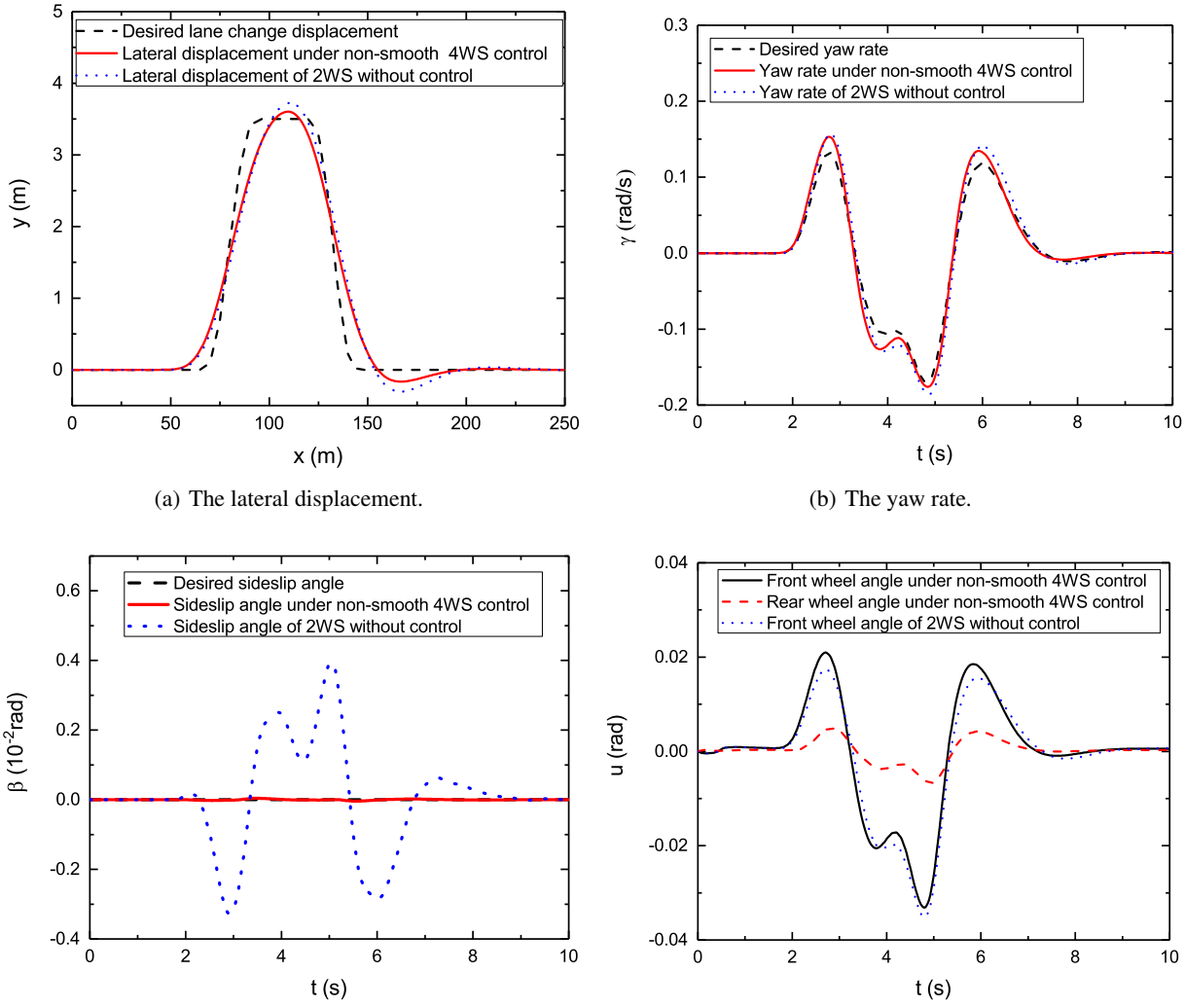

(a) The lateral displacement.

(b) The yaw rate.

(c) The sideslip angle.

(d) The wheel angle.

Fig. 4. Simulation results by the double lane closed-loop test under 90 km/h.

results of the non-smooth finite-time control method has better control effect for the active 4WS of an EV.

It should be noted that we select the linearized functions for tire forces for convenience. In fact, the tire forces are nonlinear. In the future research, we will attempt to apply nonlinear tire model into the 4WS control model to improve the control effect of the controller.

REFERENCES

[1] G.-D. Yin, N. Chen, J.-X. Wang, and J.-S. Chen, "Robust control for 4ws vehicles considering a varying tire-road friction coefficient," *International Journal of Automotive Technology*, vol. 11, no. 1, pp. 33-40, 2010.

[2] R. Marino and S. Scalzi, "Asymptotic sideslip angle and yaw rate decoupling control in four-wheel steering vehicles," *Vehicle System Dynamics*, vol. 48, no. 9, pp. 999-1019, 2010.

[3] H. Lv and S. Liu, "Closed-loop handling stability of 4ws vehicle with yaw rate control," *Strojniški vestnik-Journal of Mechanical Engineering*, vol. 59, no. 10, pp. 595-603, 2013.

[4] M. Li, Y. Jia, and J. Du, "Lpv control with decoupling performance of 4ws vehicles under velocity-varying motion," *IEEE Transactions on Control Systems Technology*, vol. 22, no. 5, pp. 1708-1724, 2014.

[5] C. Qian and W. Lin, "Smooth output feedback stabilization of planar systems without controllable/observable linearization," *IEEE Transactions on Automatic Control*, vol. 47, no. 12, pp. 2068-2073, 2002.

[6] B. Mashadi and M. Majidi, "Integrated afs/dyc sliding mode controller for a hybrid electric vehicle," *International Journal of Vehicle Design*, vol. 56, no. 1-4, pp. 246-269, 2011.

[7] F. Fahimi, "Full drive-by-wire dynamic control for four-wheel-steer all-wheel-drive vehicles," *Vehicle System Dynamics*, vol. 51, no. 3, pp. 360-376, 2013.

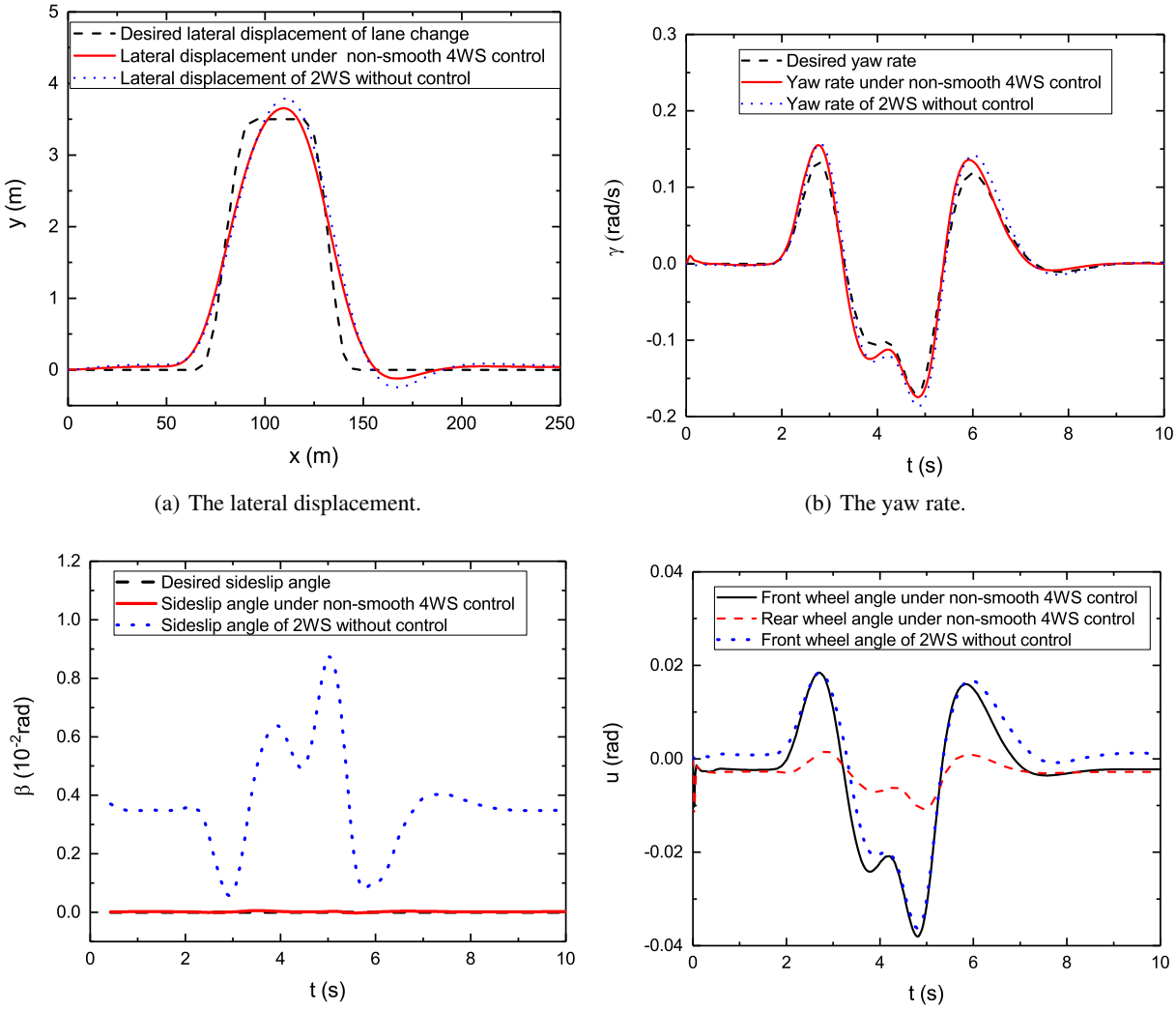

(a) The lateral displacement.

(b) The yaw rate.

(c) The sideslip angle.

(d) The wheel angle.

Fig. 5. Simulation results with lateral wind by the double lane closed-loop test under 90 km/h.

[8] Z. Shuai, H. Zhang, J. Wang, J. Li, and M. Ouyang, "Lateral motion control for four-wheel-independent-drive electric vehicles using optimal torque allocation and dynamic message priority scheduling," *Control Engineering Practice*, vol. 24, pp. 55-66, 2014.

[9] R. Wang, C. Hu, Z. Wang, F. Yan, and N. Chen, "Integrated optimal dynamics control of 4wd4ws electric ground vehicle with tire-road frictional coefficient estimation," *Mechanical Systems and Signal Processing*, vol. 60, pp. 727-741, 2015.

[10] M. Ariff, H. Zamzuri, M. Nordin, W. Yahya, S. Mazlan, and M. Rahman, "Optimal control strategy for low speed and high speed four-wheel-active steering vehicle," *Journal of Mechanical Engineering and Sciences*, vol. 8, pp. 1516-1528, 2015.

[11] A. Nasri, B. Gasbaoui, and B. M. Fayssal, "Sliding mode control for four wheels electric vehicle drive," *Procedia Technology*, vol. 22, pp. 518-526, 2016.

[12] S. Ding, L. Liu, and W. Zheng, "Sliding mode direct yaw-moment control design for in-wheel electric vehicles," *IEEE Transactions on Industrial Electronics*, vol. 64, no. 8, pp. 6752-6762, 2017.

[13] J. Yang, S. Li, and X. Yu, "Sliding-mode control for systems with mismatched uncertainties via a disturbance observer," *IEEE Transactions on Industrial Electronics*, vol. 60, no. 1, pp. 160-169, 2013.

[14] D. Ginoya, P. Shendge, and S. Phadke, "Sliding mode control for mismatched uncertain systems using an extended disturbance observer," *IEEE Transactions on Industrial Electronics*, vol. 61, no. 4, pp. 1983-1992, 2014.

[15] J. Yang, S. Li, J. Su, and X. Yu, "Continuous nonsingular terminal sliding mode control for systems with mismatched disturbances," *Automatica*, vol. 49, no. 7, pp. 2287-2291, 2013.

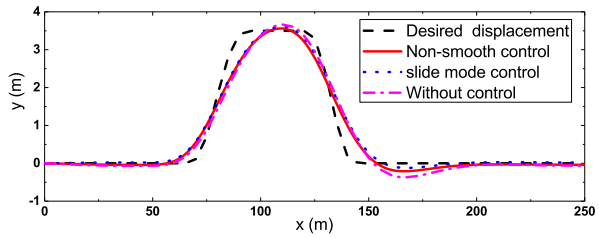

(a) The lateral displacement.

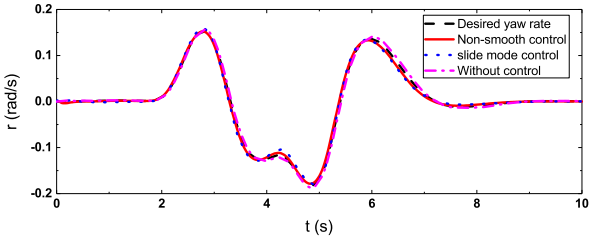

(b) The yaw rate.

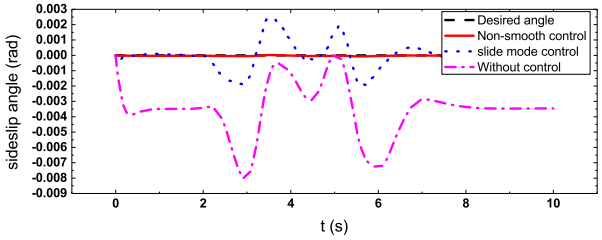

(c) The sideslip angle.

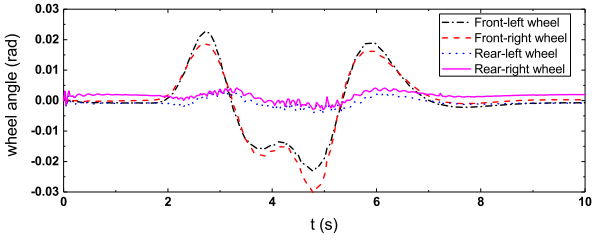

(d) The wheel angle under the slide mode control.

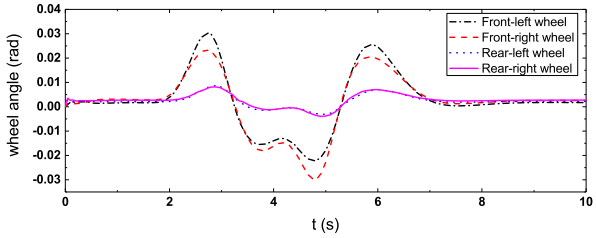

(e) The wheel angle under the non-smooth control.

Fig. 6. Simulation results for the slide mode control method and non-smooth control method.

[16] Y. Feng, X. Yu, and F. Han, "On nonsingular terminal sliding-mode control of nonlinear systems," *Automatica*, vol. 49, no. 6, pp. 1715-1722, 2013.

[17] H. Li, P. Shi, and D. Yao, "Adaptive sliding-mode control of markov jump nonlinear systems with actuator faults," *IEEE Transactions on Automatic Control*, vol. 62, no. 4, pp. 1933-1939, 2017.

[18] C. Qian and W. Lin, "Almost disturbance decoupling for a chain of power integrators perturbed by a lower-triangular vector field," in *Proceedings of the 38th IEEE Conference on Decision and Control, 1999.*, vol. 3. IEEE, 1999, pp. 2082-2087.

[19] C. Qian and L. Wei, "Homogeneity with incremental degrees and global stabilisation of a class of high-order upper-triangular systems," *International Journal of Control*, vol. 85, no. 12, pp. 1851-1864, 2012.

[20] C. Pukdeboon and P. Siricharuanun, "Nonsingular terminal sliding mode based finite-time control for spacecraft attitude tracking," *International Journal of Control, Automation and Systems*, vol. 12, no. 3, pp. 530-540, 2014.

[21] N. Wang, J.-C. Sun, and M. J. Er, "Global adaptive practical output tracking control for a class of genuinely nonlinear uncertain systems: adding an universal power integrator approach," *IEEE Access*, vol. 4, pp. 10136-10146, 2016.

[22] S. Li, H. Du, and X. Lin, "Finite-time consensus algorithm for multi-agent systems with double-integrator dynamics," *Automatica*, vol. 47, no. 8, pp. 1706-1712, 2011.

[23] X. Lin, H. Du, and S. Li, "Finite-time boundedness and l 2-gain analysis for switched delay systems with norm-bounded disturbance," *Applied Mathematics and Computation*, vol. 217, no. 12, pp. 5982-5993, 2011.

[24] H. Du, C. Qian, S. Yang, and S. Li, "Recursive design of finite-time convergent observers for a class of time-varying nonlinear systems," *Automatica*, vol. 49, no. 2, pp. 601 - 609, 2013.

[25] Z.-Y. Sun, L.-R. Xue, and K. Zhang, "A new approach to finite-time adaptive stabilization of high-order uncertain nonlinear system," *Automatica*, vol. 58, pp. 60-66, 2015.

[26] D. J. Zhao and D. G. Yang, "Model-free control of quadrotor vehicle via finite-time convergent extended state observer," *International Journal of Control, Automation and Systems*, vol. 14, no. 1, pp. 242-254, 2016.

[27] S. B. Stojanovic, D. L. Debeljkovic, and M. A. Misic, "Finite-time stability for a linear discrete-time delay systems by using discrete convolution: An lmi approach," *International Journal of Control, Automation and Systems*, vol. 14, no. 4, pp. 1144-1151, 2016.

[28] C.-C. Chen, C. Qian, X. Lin, Z.-Y. Sun, and Y.-W. Liang, "Smooth output feedback stabilization for a class of nonlinear systems with time-varying powers," *International Journal of Robust and Nonlinear Control*, 2017.

[29] Y. Wei, J. Qiu, and H. R. Karimi, "Reliable output feedback control of discrete-time fuzzy affine systems with actuator faults," *IEEE Transactions on Circuits & Systems I Regular Papers*, vol. 64, no. 1, pp. 170-181, 2017.

[30] Y. Wei, J. Qiu, H. K. Lam, and L. Wu, "Approaches to t-s fuzzy-affine-model-based reliable output feedback control for nonlinear ito stochastic systems," *IEEE Transactions on Fuzzy Systems*, vol. 25, no. 3, pp. 569-583, 2017.

[31] Y. Wei, J. Qiu, H. R. Karimi, and M. Wang, "New results on h ∞ dynamic output feedback control for markovian jump systems with time-varying delay and defective mode information," *Optimal Control Applications & Methods*, vol. 35, no. 6, pp. 656-675, 2015.

[32] Y. Wei, J. Qiu, and S. Fu, "Mode-dependent nonrational output feedback control for continuous-time semi-markovian jump systems with time-varying delay," *Nonlinear Analysis Hybrid Systems*, vol. 16, pp. 52-71, 2015.

Qinghua Meng was born in 1977. He received the Ph.D. degree from Zhejiang University, China, in 2005. Since 2005, he has been with the School of Mechanical Engineering, Hangzhou Dianzi Universit, where he is now an Associate Professor. His current research interests include electric vehicle stability control, and Mechanical fault diagnosis and signal processing.

Zong-Yao Sun was born in 1979. He received the Ph.D. degree from Shandong University, China, in 2009. Since 2009 he has been with the Institute of Automation, Qufu Normal University, where he is now an associate Professor. His current research interests include nonlinear control, adaptive control.

Yushan Li was born in 1970. He received the Ph.D. degree from Shandong University of Science and Technology, China, in 2011. He now works in the College of Transportation, Shandong University of Science and Technology, where he is now an associate Professor. His current research interests include vehicle control and vehicle driverless technology.